

Dynamics of Water Confined in the Interdomain Region of a Multidomain Protein[†]

Lan Hua,[‡] Xuhui Huang,[‡] Ruhong Zhou,^{‡,§} and B. J. Berne^{*,‡,§}

Department of Chemistry, Columbia University, New York, New York 10027, and Computational Biology Center, IBM Thomas J. Watson Research Center, 1101 Kitchawan Road, Yorktown Heights, New York 10598

Received: September 22, 2005; In Final Form: November 11, 2005

Molecular dynamics simulations are performed to study the dynamics of interfacial water confined in the interdomain region of a two-domain protein, BphC enzyme. The results show that near the protein surface the water diffusion constant is much smaller and the water–water hydrogen bond lifetime is much longer than that in bulk. The diffusion constant and hydrogen bond lifetime can vary by a factor of as much as 2 in going from the region near the hydrophobic domain surface to the bulk. Water molecules in the first solvation shell persist for a much longer time near local concave sites than near convex sites. Also, the water layer survival correlation time shows that on average water molecules near the extended hydrophilic surfaces have longer residence times than those near hydrophobic surfaces. These results indicate that local surface curvature and hydrophobicity have a significant influence on water dynamics.

1. Introduction

Water plays a central role in the structure, thermodynamics, stability, functionality, and kinetics of large water soluble proteins.¹ The biological activity of these molecules generally occurs within a relatively narrow range of temperatures, solvent chemical potentials, and ionic concentrations. Most cellular functions are driven not by temperature gradients but by changes in solvent environment.^{1,2} To understand the kinetics of hydrophobic collapse and molecular self-assembly, one must grapple with water dynamics near the extended nonpolar surfaces of proteins. The aggregation and subsequent removal of such surfaces from contact with water are of particular interest.^{3–13} Quantitative understanding of the hydrophobic effect and associated water dynamics near the extended hydrophobic surfaces of biomolecules remains a daunting problem due to the inherently complex nature of the systems. In this paper, we explore the dynamics of water near the hydrophobic surface in the interdomain region of a specific protein.

The structural and dynamical properties of water molecules in the first hydration shell of peptides and proteins are of special importance.^{12,14–19} Experimental techniques, such as high-resolution X-ray and neutron diffraction,^{20,21} NMR methods,²² and femtosecond fluorescence,²³ have been used to study the properties of water around proteins. Probing dynamic properties such as interfacial water hydrogen bond lifetimes remains a challenge in experiments. Molecular dynamics simulations, on the other hand, provide a powerful theoretical tool for the study of hydrogen bond kinetics and other dynamic processes near proteins. Much work has been done by various groups^{6,12,24–31} on water dynamics around single proteins or peptides; for example, Xu and Berne found that water hydrogen bonds live longer in the first solvation shell of a 16-residue polypeptide than in bulk water.¹⁴

Zhou et al.²⁴ recently examined how water molecules mediate the hydrophobic collapse of the BphC enzyme protein,²⁴ a two-domain protein, and found that liquid water persisted in the interdomain region with a density 10–15% lower than that in the bulk even at small domain separations. Water depletion and hydrophobic collapse occurred on a nanosecond time scale, fully 1 or 2 orders of magnitude slower than that found by simulation in the collapse of idealized paraffin-like plates.^{32,33} In this paper, we focus on water dynamics in the interdomain region of this same two-domain protein, BphC enzyme, as a function of the distance from the domain interface. We find that dynamics of water molecules proximate to the domain interfaces is significantly slower than in bulk. Furthermore, water molecules next to concave regions of the surface persist for an extremely long time (up to 200 ps), much longer than near convex regions (up to 25 ps). Also, water molecules near the extended hydrophilic regions of the surface have longer residence time than those near hydrophobic regions of the surface. These results indicate that local surface curvature and hydrophobicity can have a significant influence on water dynamics.

This paper is organized as follows. In section 2, the system is defined and the methods used to simulate this system are presented. In section 3, the results for different dynamic properties are discussed. In section 4, a short summary and conclusion is presented.

2. System and Methods

The system studied in this paper, the BphC enzyme of KKS102 (see Figure 1a), a two-domain protein, is the same system in which we studied hydrophobically induced collapse in a previous paper.²⁴ This two-domain protein was selected on the basis of the spatial hydrophobicity profiling on all multidomain proteins in the Protein Data Bank (PDB).^{24,34} The BphC enzyme (2,3-dihydroxybiphenyl dioxygenase) is a key enzyme in degrading toxic polychlorinated biphenyls. It is an oligomeric enzyme made up of eight identical subunits each of 292 amino acid residues. Each subunit consists of two domains: domain 1 (N-terminal part, residues 1–135) and domain

[†] Part of the special issue “Michael L. Klein Festschrift”.

^{*} To whom correspondence should be addressed. E-mail: berne@chem.columbia.edu.

[‡] Columbia University.

[§] IBM Thomas J. Watson Research Center.

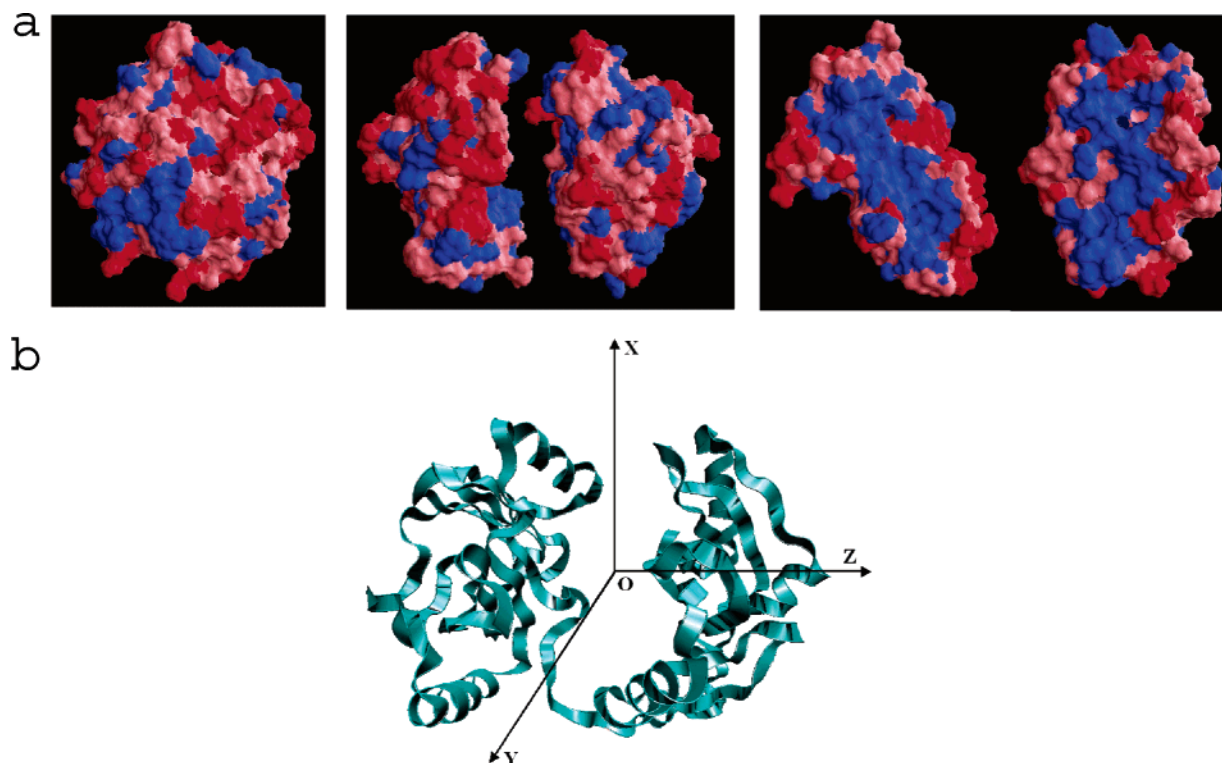


Figure 1. Two-domain protein BphC enzyme (PDB entry 1dhy). (a, left) Molecular surface of the folded complex (the domain interfaces are buried) with hydrophobic residues (I, F, V, M, W, C, and Y) colored blue, strong hydrophilic residues (K, D, E, R, Q, and N) colored red, and weak hydrophilic residues colored pink. (a, middle) The two domains are separated by 12 Å along the line of the two domain centers so the interface can be seen. (a, right) The two domains are separated and also rotated such that the interface areas are facing the reader. Large hydrophobic surface areas can be seen on the domain boundary. (b) Solvated protein system in water with the interdomain gap distance D equal to 6 Å. These images are generated with PPV⁴⁸ and VMD.⁴⁹

2 (C-terminal part, residues 136–292). In this paper, only one subunit (two domains) is included and we refer to it as a two-domain protein. The focus will be on the water mobility or dynamics near the interface of the interdomain region.

The starting structure in our simulation is taken from the crystal structure deposited in PDB (entry 1dhy). The interdomain distance of the crystal structure is increased by D along the direction of the vector connecting the two domain centers to create “gaps” between the two domains (to make room for water). In the previous study,²⁴ many D values, ranging from 2.5 Å (which can barely hold one layer of water) to 20 Å, were used. In this study, a few representative D values, such as 4, 12, and 20 Å, are used (other D values were also tried, and similar results were obtained). The resulting protein configurations are then solvated in a water box, with water layers at least 8 Å from the protein surfaces. Eight Na⁺ counterions are added to neutralize each solvated system. The solvated protein systems have up to 42 000 atoms (the actual size varies for different interdomain distances). The GROMACS simulation package is used here for this large system because of its fast speed,³⁵ with the OPLSAA force field for the protein³⁶ and SPC water model for the explicit solvent.³⁷ For the long-range electrostatic interactions, the Particle Mesh Ewald (PME) method is used. For the van der Waals interactions, a 13 Å cutoff is used. A time step of 1.0 fs is used with the LINCS bond length constraint algorithm.³⁸

A standard equilibration procedure is used to equilibrate each solvated system before data collection: a conjugate gradient minimization followed by a 200 ps NPT simulation is performed for each solvated system. A 500 ps NPT run is made to sample a set of initial states for the subsequent NVE simulations. The NVE trajectories are used to calculate the various time correla-

tion functions. This approach prevents the fictitious dynamics in NPT simulations arising from the fictitious degrees of freedom in the temperature and pressure control. In all these MD simulations, the two-domain protein is restrained in space with a force constant of 10 kJ mol⁻¹ Å⁻².

3. Results and Discussion

It was shown in our previous work²⁴ that attractive interactions, particularly electrostatic interactions between protein and water, can have a profound effect on hydrophobic collapse and the water drying transition. When the two-domain protein (with each already formed domain) collapses into the final globular structure, water molecules in the interdomain region exhibit interesting properties.²⁴ Liquid water persisted in the interdomain region with a density 10–15% lower than in the bulk, even at small domain separations. Water depletion and hydrophobic collapse occurred on a nanosecond time scale, fully 1 or 2 orders of magnitude slower than that found by simulation in the collapse of idealized paraffin-like plates.³² These findings show that realistic solute–water forces play a significant role in hydrophobic collapse. It is worth investigating the water behavior near the interfacial region in greater detail, such as the water mobility, hydrogen bond relaxation time, water residence time near concave or convex surfaces, water radial distribution functions, etc.

As described in the previous section, the coordinate system for the solvated two-domain BphC enzyme is defined such that the vector connecting the two domain centers of mass (COM) serves as the z -direction and the midpoint between the COM of the two domains serves as the origin. The region between the two domains can then be subdivided into parallel layers that are Δz thick with faces perpendicular to z (along the x – y plane;

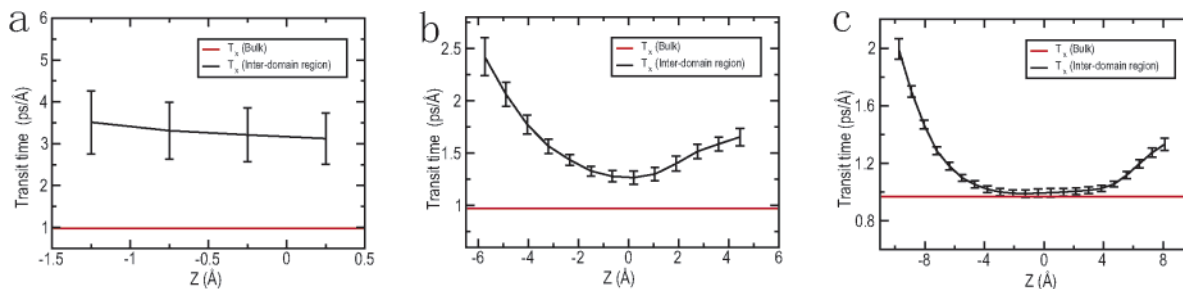


Figure 2. (a) Water transit time (time needed to have a 1 \AA^2 mean-square displacement) along the z axis in the interdomain region when $D = 4 \text{ \AA}$. The error bar is computed from 10 different 500 ps NVE simulations. (b) Same as panel a except $D = 12 \text{ \AA}$. (c) Same as panel a except $D = 20 \text{ \AA}$.

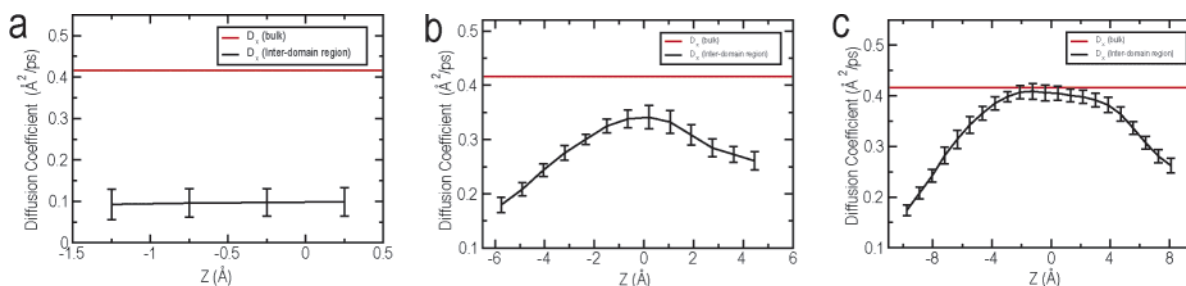


Figure 3. (a) Water diffusion constant which is estimated from the Einstein equation along the z axis in the interdomain region when $D = 4 \text{ \AA}$. The error bar is computed from 10 different 500 ps NVE simulations. (b) Same as panel a except $D = 12 \text{ \AA}$. (c) Same as panel a except $D = 20 \text{ \AA}$.

see Figure 1b). Within this coordinate system, for example, the interdomain region can be roughly described as follows: $-8 \text{ \AA} < x < 8 \text{ \AA}$, $-8 \text{ \AA} < y < 8 \text{ \AA}$, and $-6 \text{ \AA} < z < 6 \text{ \AA}$ when $D = 12 \text{ \AA}$. Almost all the water properties obtained below will be described as a function of z within the interdomain region.

Transit Time and Diffusion Constant. It is expected that the water molecules might diffuse more slowly near domain interfaces than in bulk water due to hydrophobic and surface curvature effects.^{12,14} However, to accurately obtain the diffusion constants in the nonuniform environment, one needs to solve the Smoluchowski equation³⁹ for regions with non-zero potential of mean force, such as water–vapor interfaces or the current confined water (more discussions below).⁴⁰ Thus, we use a simpler measure, the water “transit time”, which is defined as the time required for the mean-square displacement (MSD) of a water molecule to be 1 \AA^2 . Here we define the MSD to be

$$\langle \Delta x(\tau)^2 \rangle = \frac{1}{T} \sum_{\tau=0}^T \frac{1}{N(t) < i=1} \sum_{i=1}^{N(t)} [x_i(t + \tau) - x_i(t)]^2 \quad (1)$$

where $N(t)$ is the number of water molecules in a specified x – y slab (layer parallel to the domain interfaces) at time t . This measures the displacement (transverse to z) of water molecules initially in the specified layer. Figure 2 shows the transit time for water molecules as a function of z for the three domain separations ($D = 4, 12,$ and 20 \AA) given in panels a–c, respectively. Each data point is averaged over a layer that is 3.5 \AA thick (z -axis) so that there are enough water molecules for averaging. The error bars are computed from ten 500 ps NVE simulations starting from different initial configurations. Using the $D = 12 \text{ \AA}$ case for illustration, the shortest transit time is found to be $1.27 \pm 0.06 \text{ ps}$ near the center of the interdomain region ($z = 0 \text{ \AA}$) and the longest one is found to be $2.42 \pm 0.18 \text{ ps}$ at the left-hand side domain interface ($z = -5.75 \text{ \AA}$). It is interesting to note that the longest transit time can be as much as 1.91 times the shortest. Thus, the domain interfaces do have a significant effect on the water mobility.

For a comparison, the bulk transit time is found to be approximately 0.97 ps . It is also interesting to note that water molecules near the interface on the left ($z = -5.75 \text{ \AA}$) have a transit time $\sim 47\%$ longer than the interface on the right ($z = 4.45 \text{ \AA}$), which suggests that the difference in the average hydrophobicity and curvature can have a significant effect on water dynamics. The results for the domain separation of 20 \AA show similar effects except that in this case the transit time for water at the center of the interdomain region is close to that of bulk water, indicating that for a 20 \AA gap the central waters are bulklike. When $D = 4 \text{ \AA}$, water molecules in different layers inside the interdomain region show roughly the same transit time, which is not too surprising given the narrow size of the interdomain region. The water molecules near the interface exhibit a slightly longer transit time than that in the $D = 12 \text{ \AA}$ case, indicating that both domain interfaces have contributed to the slower mobility of water molecules.

Pu et al.⁴⁰ presented a method for determining diffusion coefficients of solvent near interfaces, a method which requires accurate knowledge of the solvent–solute potential of mean force, a quantity difficult to determine for the rough and irregular surfaces of our two-domain protein. However, a rough estimate of the diffusion coefficient as a function of distance along z , $D_x(z)$, can be obtained from the Einstein relation assuming the potential of mean force caused by the two domain surfaces is reasonably small:

$$\langle \Delta x(z, t)^2 \rangle = 2D_x(z)t \quad (2)$$

Figure 3 shows this diffusion constant for the three interdomain separations ($D = 4, 12,$ and 20 \AA). Obviously, with this simple approach, the diffusion constant and the above transit time are inversely related. For completeness, we include the more commonly used diffusion constants here as well. To avoid contributions from the short-time ballistic motion, MSD data between 2 and 4 ps were used to fit eq 2; see Figure 4a for details. Consistent with the water transit times given above, we find that water molecules near the domain interfaces diffuse

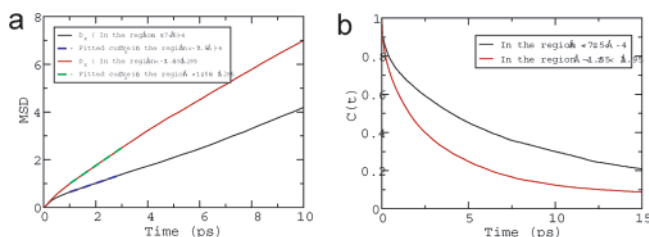


Figure 4. (a) Two example MSDs with time for the interdomain regions defined by $-7.5 \text{ \AA} < z < -4 \text{ \AA}$ and $-1.55 \text{ \AA} < z < 1.95 \text{ \AA}$. (b) Two example hydrogen bond correlation times for the interdomain regions defined by $-7.5 \text{ \AA} < z < -4 \text{ \AA}$ and $-1.55 \text{ \AA} < z < 1.95 \text{ \AA}$.

much slower than those near the center of the interdomain region, as expected. For example, when $D = 12 \text{ \AA}$ (see Figure 3b), the diffusion constant is found to be largest ($D_x = 0.341 \pm 0.021 \text{ \AA}^2/\text{ps}$) near the center of the interdomain region ($z = 0 \text{ \AA}$) and smallest ($D_x = 0.179 \pm 0.013 \text{ \AA}^2/\text{ps}$) near the left domain when $z = -5.75 \text{ \AA}$. Again the diffusion coefficient varies by a factor of 2 in going from the protein surface to the center of the interdomain region. For comparison, the bulk diffusion constant is found to be $0.416 \pm 0.040 \text{ \AA}^2/\text{ps}$ (this is slightly larger than the previously reported result due to short cutoffs used in the previous simulation⁴¹). The diffusion constant near the left-hand side interface ($z = -5.75 \text{ \AA}$) is also 46% smaller than that near the right-hand side interface ($z = 4.45 \text{ \AA}$). Again, the results from the larger interdomain separation ($D = 20 \text{ \AA}$) are similar to those for the intermediate separation ($D = 12 \text{ \AA}$) except that the water at the center of interdomain region behaves in a bulklike manner (see Figure 3c). The water diffusion constant inside the interdomain region when $D = 4 \text{ \AA}$ has a value of $\sim 0.1 \text{ \AA}^2/\text{ps}$ at all layers. Since only fewer than two layers of water molecules can fit in the interdomain region when $D = 4 \text{ \AA}$, the water molecules diffuse more slowly than those with larger separations due to attractions from both sides of the domain interface (see Figure 3a). When $D = 4 \text{ \AA}$, water diffusion in the confined region is also much slower than that at a single domain surface.

The large variation in water diffusion constant and transit time with distance from the interface indicates that the hydrophobic interfaces of proteins have a significant effect on the water mobility.

Hydrogen Bond Relaxation Time. Water–water hydrogen bond lifetimes should be different for water proximate to protein domains and for water in bulk. The relaxation time of the water–water hydrogen bonds can be characterized by the hydrogen bond autocorrelation function:^{14,42}

$$c(t) = \langle h(0)h(t) \rangle / \langle h(0)h(0) \rangle \quad (3)$$

where $h(t) = 1$ if a pair of targeted waters is hydrogen bonded at time t and $h(t) = 0$ otherwise. A geometric definition is used for water–water hydrogen bonds. Two water molecules are considered to be hydrogen bonded if their inter-oxygen distance is no greater than 3.5 \AA and the angle between the O–O axis and one of the O–H bonds is no greater than 30° .⁴² Figure 4b shows two examples of autocorrelation functions for two layers of water inside the interdomain region. The relaxation time of hydrogen bonds (τ_{HB}) can then be obtained by setting the autocorrelation function to $c(\tau_{\text{HB}}) = e^{-1}$.

The hydrogen bond relaxation time as a function of z in the interdomain region is shown in Figure 5. The water–water hydrogen bonds near the interdomain surfaces have longer relaxation times than those near the center of the interdomain region. When $D = 12 \text{ \AA}$, the longest relaxation time ($7.06 \pm$

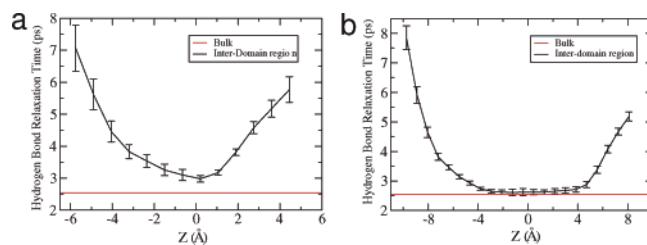


Figure 5. (a) Water hydrogen bond relaxation time along the z axis in the interdomain region when $D = 12 \text{ \AA}$. The error bar is computed from 10 different 500 ps NVE simulations. (b) Same as panel a except $D = 20 \text{ \AA}$.

0.72 ps) is found for water molecules near the left domain interface while the shortest relaxation time ($2.97 \pm 0.10 \text{ ps}$) is found for water molecules near the center of the interdomain region, with the longest being 2.4 times greater than the shortest. Interestingly, the relaxation times near the left protein domain interface are $\sim 23\%$ longer than that near the right domain interface due to the different surface features. These results show trends similar to those found for the water transit time and for the self-diffusion constant. As in the case of the transit times and diffusion coefficients, hydrogen bonds near the center of the interdomain region have longer lifetimes than in bulk water when $D = 12 \text{ \AA}$ but have ones comparable to that of bulk water when $D = 20 \text{ \AA}$, indicating the surface effect can reach beyond 6 \AA . Detailed results from the $D = 20 \text{ \AA}$ case indicate that the surface effect on hydrogen bond lifetime can in fact reach as far as 8 \AA . Thus, in the two-domain protein, it appears that the presence of the two surfaces affects the water molecules that are farther from the surface than only one isolated domain. For example, studies of hydrogen bond lifetime near single surfaces show that water dynamics is affected out to a distance of $4\text{--}5 \text{ \AA}$,²⁵ rather than out to 8 \AA in the two-domain case presented here. The hydrogen bond lifetime near the single domain surface is smaller than that in the confined region between the two domains.

The long-time decay of the hydrogen bond correlation function, for times longer than $\sim 1 \text{ ps}$, could be related to the translational pair diffusion of water.¹⁴ This pair diffusion, like the self-diffusion above, is slower in the solvation shell of the protein with the consequence that, for water in this region, the observed deceleration of the long-time decay of the hydrogen bond correlation function is at least partly due to the deceleration of the water pair diffusion. To eliminate the contributions from pair diffusion, one can calculate the following correlation function¹⁴

$$O(t) = \langle h(0)[1 - h(t)]H(t) \rangle / \langle h(0)h(0)H(t) \rangle \quad (4)$$

where $H(t) = 1$ if the pair of water molecules are closer than 3.5 \AA at time t and $H(t) = 0$ otherwise. Thus, $O(t)$ is the conditional probability that a hydrogen bond is broken at time t given that the involved pair of water molecules have not diffused away; thus, it reflects the making and breaking of bonded or soon to be bonded water pairs. Figure 6 shows $O(t)$ values for various water layers starting near the left domain interface for an interdomain separation of 12 \AA . Significant differences from the bulk can be seen for water near the domain interface. The closer the water is to the domain interface, the more slowly its hydrogen bonds break. It should be noted that in the z region between -1.55 and 1.95 \AA , hydrogen bonds have the same probability to break by reorienting as they do in

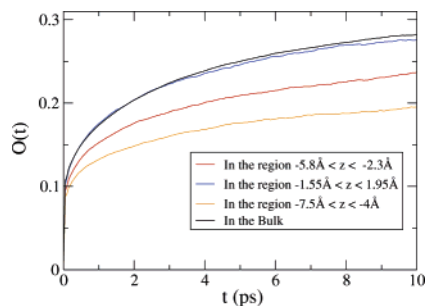


Figure 6. Conditional time-dependent probability of breaking hydrogen bonds, $O(t)$ (see eq 4), in different environments.

bulk. Thus, the longer hydrogen bond lifetimes near the center of the two-domain region are mainly due to the pair translational diffusion.

Solvent Structure and Residence Times of Water near Local Surfaces. So far, all of the water dynamic properties are calculated as a function of the distance from the domain surfaces, which are averaged over a water layer of $16 \text{ \AA} \times 16 \text{ \AA} \times 3.5 \text{ \AA}$ (a thickness of 3.5 \AA). These data are very useful in providing the overall surface effects; however, they do not offer a detailed picture of water behavior near various local surface regions, such as convex or concave sites, and hydrophobic or hydrophilic sites. To address such sensitivity, one way is to calculate local properties such as the radial distribution function of water oxygen atoms around the different protein atomic sites R . These functions can be defined as

$$g(r;R) = \frac{\bar{N}(r;R)}{4\pi\rho(R)r^2 dr} \quad (5)$$

where $\bar{N}(r;R)$ is the average coordination number between r and $r + dr$ around protein atomic site R

$$\bar{N}(r;R) = \frac{1}{T} \sum_{t=0}^T N[r;R(t)] \quad (6)$$

in which $N[r;R(t)]$ is the number of water oxygen atoms between r and $r + dr$ around atomic site R at time t . And ρ is the average density of water oxygen atoms around the protein atom site R within the volume defined by a sphere

$$\rho(R) = \frac{1}{VT} \sum_{t=0}^T N[R(t)] \quad (7)$$

Representative radial distribution functions are shown in Figure 7. Several interesting features emerge. (1) There is a clear difference between the water solvation shell structure around hydrophobic (apolar) and hydrophilic (polar) atoms, as shown in Figure 7a. The water solvent molecules around apolar atoms have a broader distribution with peaks near $3.5\text{--}4 \text{ \AA}$, while water molecules around polar atoms have distributions with peaks near $2.7\text{--}3 \text{ \AA}$. (2) The atomic sites inside concave regions generally have broader distributions and lower peak heights than those in the convex regions (see Figure 7b), probably because concave atomic sites are more shielded by other surrounding protein atoms. Here the concave and convex sites are picked manually on the basis of the local surface curvature.⁶ These results are generally consistent with previous findings by Bizzarri et al. with a different protein plastocyanin, a copper-containing protein involved in photosynthesis.¹²

It is also of interest to compute the water residence time of water molecules proximate to various local atomic sites on the

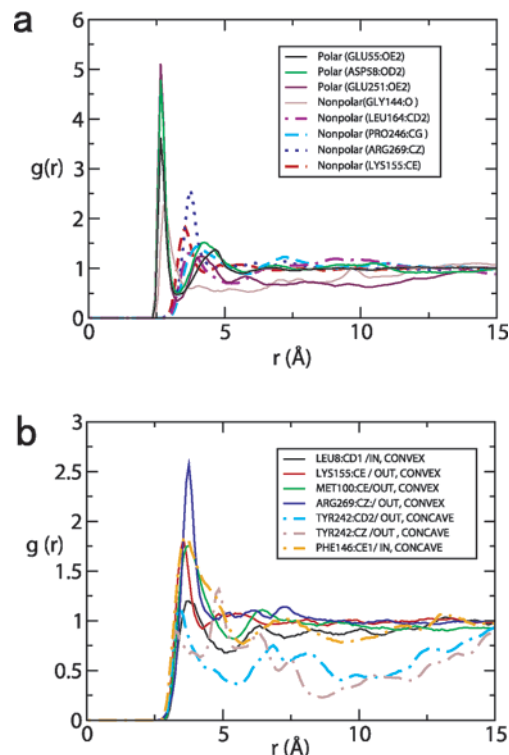


Figure 7. Water radial distribution function when $D = 12 \text{ \AA}$ in the first solvation shell of nonpolar vs polar sites (a) and concave vs convex surfaces (b).

domain surfaces. This can help us to understand different water behavior due to local topology, hydrophobicity, and polarity at various sites. It can also be used to compare overall atomic sites inside and outside the interdomain region. The residence time can be determined from a survival time correlation function $C(t)$, which describes the relaxation of the hydration shell near any atomic site.^{12,43} For a given atomic site α in the protein, $C_\alpha(t)$ can be defined in terms of a binary function $p_{\alpha,j}(t', t'+t; t_0)$,¹² which takes a value of 1 if the j th water molecule stays in the coordination shell of atomic site α at both time steps t' and $t' + t$ and in the interim does not leave for any continuous period longer than t_0 (here $t_0 = 2 \text{ ps}$, and this t_0 means not to count the leave if the water molecules quickly return to the solvation shell).¹² Otherwise, it takes the value of zero. Thus, $C_\alpha(t)$ can be expressed as^{12,43}

$$C_\alpha(t) = \frac{1}{N_w} \sum_{j=1}^{N_w} \sum_{t'=0}^T p_{\alpha,j}(t', t'+t; t_0) \quad (8)$$

where N_w is the total number of water molecules in the system.

It is found that the survival time correlation function eq 8 can be best fit with a double exponential

$$C_\alpha(t) = Ae^{-(t/\tau_s)} + Be^{-(t/\tau_l)} \quad (9)$$

where τ_s and τ_l are the short and long time decay constants, respectively. These decay times correspond to water molecules that stay in the hydration shell for prolonged periods of time (τ_l) or enter and leave shortly (τ_s). Tables 1–3 list the short and long water residence times for some representative atomic sites. Even though the detailed numbers can differ by a wide margin within the same category, there are still some general conclusions to be made. On average, the concave sites have significantly longer residence times than the convex sites. Meanwhile, the sites inside the interdomain gap have slightly

TABLE 1: Water Residence Time at Various Atomic Sites (concave vs convex)

atom no.	description	first shell (Å)	τ_s	τ_l
Concave				
2164	Gly144 O	3.65	1.88	45.85
3124	Met204 O	3.26	0.11	142.06
3695	Tyr242 CD2	5.56	0.10	124.61
3701	Tyr242 CZ	4.16	0.07	36.29
2194	Phe146 CE1	5.47	14.28	83.70
10	Ser1 OG	3.66	9.49	178.87
Convex				
647	Gln44 OE1	3.05	0.11	19.49
2477	Leu164 CD2	5.27	0.06	13.24
1654	Phe109 CZ	5.46	0.96	14.50
3027	Arg199 NH1	3.15	0.09	14.17
4120	Arg269 CZ	4.65	1.57	18.55
4124	Arg269 NH2	3.15	0.10	9.93
1220	Gln81 OE1	3.36	1.05	11.25
830	Glu55 OE2	3.16	0.09	14.00
1894	His124 O	3.45	1.19	9.23
128	Leu8 CD1	5.09	0.12	13.08
4169	Met272 O	3.36	0.11	8.06
1648	Phe109 CD2	4.27	1.32	15.27
334	Phe21 CZ	5.56	1.10	16.33
403	Ser25 O	3.36	0.12	8.17
2088	Thr138 OG1	4.47	1.98	23.40
2425	Thr161 OG1	3.41	0.10	22.11
4019	Thr263 OG1	3.65	1.72	18.71
1295	Thr87 OG1	3.67	0.10	18.94
3282	Tyr215 OH	3.38	1.11	11.35

TABLE 2: Water Residence Times at Various Atomic Sites (inside vs outside)

atom no.	description	first shell (Å)	τ_s	τ_l
Inside				
647	Gln44 OE1	3.05	0.11	19.49
2164	Gly144 O	3.65	1.88	45.85
85	Leu5 CD2	5.96	1.64	22.75
3124	Met204 O	3.26	0.11	142.06
3734	Thr245 OG1	3.35	2.00	43.93
3027	Arg199 NH1	3.15	0.09	14.17
1621	Asp107 OD2	3.26	2.00	33.23
873	Asp58 OD2	3.26	0.11	17.73
128	Leu8 CD1	5.09	0.12	13.08
2194	Phe146 CE1	5.74	14.28	83.70
334	Phe21 CZ	5.56	1.10	16.33
3748	Pro246 CG	5.79	2.00	29.20
Outside				
4120	Arg269 CZ	4.65	1.57	18.55
4124	Arg269 NH2	3.15	0.10	9.93
2617	Asp173 O	3.46	0.53	18.24
3829	Glu251 OE2	3.26	1.05	57.33
830	Glu55 OE2	3.16	0.09	14.00
1519	Met100 O	3.65	0.07	13.86
4169	Met272 O	3.36	0.11	8.06
2425	Thr161 OG1	3.41	0.10	22.11
4019	Thr263 OG1	3.65	1.72	18.71
1295	Thr87 OG1	3.67	0.10	18.94
3282	Tyr215 OH	3.38	1.11	11.35
4231	Lys276 CE	4.57	1.65	17.81
4257	Val278 CG1	5.47	0.10	29.98

longer residence times than the sites outside the gap. Surprisingly, the apolar sites have residence times comparable to those of the polar sites, probably because of the complex nature of the neighboring sites in terms of atomic hydrophobicity. It should be pointed out that the polar and nonpolar sites selected here are mostly in the outside domain interface region. For atoms with high solvent accessibility, either polar or apolar, they are surrounded by many water molecules rapidly exchanging with bulk solvent, which might result in a similar residence time as pointed out by Luise et al.,²⁷ as well. Interestingly, others have

TABLE 3: Water Residence Times at Various Atomic Sites (polar vs nonpolar)

atom no.	description	first shell (Å)	τ_s	τ_l
Polar				
647	Gln44 OE1	3.05	0.11	19.49
3734	Thr245 OG1	3.35	2.00	43.93
3702	Tyr242 OH	3.16	0.11	40.54
3027	Arg199 NH1	3.15	0.09	14.17
4124	Arg269 NH2	3.15	0.10	9.93
1621	Asp107 OD2	3.26	2.00	33.23
2617	Asp173 O	3.46	0.53	18.24
1220	Gln81 OE1	3.36	1.05	11.25
3829	Glu251 OE2	3.26	1.05	57.33
830	Glu55 OE2	3.16	0.09	14.00
1894	His124 O	3.45	1.19	9.23
1519	Met100 O	3.65	0.07	13.86
4169	Met272 O	3.36	0.11	8.06
403	Ser25 O	3.36	0.12	8.17
2088	Thr138 OG1	4.47	1.98	23.40
2425	Thr161 OG1	3.41	0.10	22.11
4019	Thr263 OG1	3.65	1.72	18.71
1295	Thr87 OG1	3.67	0.10	18.94
3282	Tyr215 OH	3.38	1.11	11.35
Nonpolar				
2477	Leu164 CD2	5.27	0.06	13.24
1514	Met100 CE	5.44	2.00	24.16
1654	Phe109 CZ	5.46	0.96	14.50
4120	Arg269 CZ	4.65	1.57	18.55
128	Leu8 CD1	5.09	0.12	13.08
1648	Phe109 CD2	4.27	1.32	15.27
334	Phe21 CZ	5.56	1.10	16.33
4231	Lys276 CE	4.57	1.65	17.81
4257	Val278 CG1	5.47	0.10	29.98
4164	Met272 CE	5.47	0.10	20.75
828	Glu55 CD	4.06	0.10	19.83
1353	Glu91 CG	5.43	2.00	35.33
1195	Arg80 CD	4.96	2.00	33.01
1957	Leu128 CD2	5.34	1.89	18.63
1887	His124 CD2	5.17	0.09	11.88

observed the following ranking relationship for τ (τ_l) for many proteins such as crambin,⁴⁴ plastocyanin,⁴⁵ and azurin.²⁷ $\tau_{\text{charged}} > \tau_{\text{polar}} > \tau_{\text{nonpolar}} \approx \tau_{\text{bulk}}$. However, for bovine pancreatic trypsin inhibitor (BPTI), such a relationship among polar, charged, and nonpolar residues was not observed.^{28,46} It might be expected that the residence times should be somehow controlled by H-bond network dynamics; nevertheless, a simple correlation between τ and the average lifetime of H-bonds (τ_{rlx}) has not been found.^{45,46}

As mentioned above, it is somewhat surprising to notice that the hydrophobic and hydrophilic sites exhibit comparable water residence times. We suspect that the residence times near hydrophobic and hydrophilic sites are largely influenced by neighboring opposite sites in terms of hydrophobicity. Furthermore, these atomic hydrophobic or hydrophilic sites can be overrun by local convex or concave geometries. To simplify the complication, we calculate the averaged residence time over a larger area instead of individual atomic sites by realizing the fact that the domain interface region is largely hydrophobic while the outside domain interface region is largely hydrophilic.

Thus, similarly, we can define the “layer” survival time correlation function $C_R(t)$

$$C_R(t) = \sum_{j=1}^{N_w} \frac{1}{T} \sum_{t'=0}^T p_{R,j}(t', t'+t) \quad (10)$$

where $p_{R,j}(t', t'+t)$ is a binary function that takes a value of 1 if the j th water molecule stays in a confined region with thickness R from t' to $t' + t$ without escaping during this interval. This

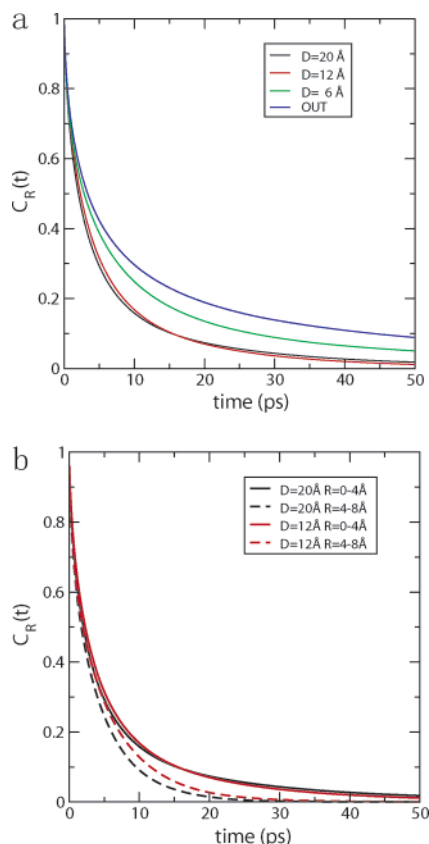


Figure 8. (a) Water layer survival correlation time function $C_R(t)$ for water molecules in various first solvation shells. The blue line represents the outside domain interface region ($-12 \text{ \AA} < x < 12 \text{ \AA}$, $-12 \text{ \AA} < y < 12 \text{ \AA}$, and up to 4 \AA from the protein surface), which is largely hydrophilic. The other lines all represent the interdomain region but with different domain separations D , which are largely hydrophobic. (b) Comparison of the layer survival correlation time for the first (0–4 Å) and second (4–8 Å) solvation shells. The correlation time of the first solvation shell decays slower than that of the second solvation shell, indicating an enhanced immobility of water near the domain surfaces.

quantity, $C_R(t)$, measures the probability that a water molecule remains in a given region for a certain time t , without ever exchanging with the bulk water.⁴⁷

Figure 8a shows this layer survival correlation time for a few representative cases from the protein surface with a thickness of 4 \AA (defined as the first solvation shell). The blue line represents the outside domain interface region ($-12 \text{ \AA} < x < 12 \text{ \AA}$, $-12 \text{ \AA} < y < 12 \text{ \AA}$, and up to 4 \AA from protein surface), which is largely hydrophilic. The other lines all represent the interdomain region but with different domain separations D , which are largely hydrophobic. The blue curve decays slower than all the other curves, indicating that on average water molecules in the first solvation shell of the hydrophilic surface have residence times longer than that of the hydrophobic surface. The black ($D = 20 \text{ \AA}$) and red ($D = 12 \text{ \AA}$) curves decay at almost the same rate, indicating that when the domain separations increase to a certain value the effect from the opposite domain interface is essentially negligible. However, at a smaller separation, such as $D = 6 \text{ \AA}$ (green line), the effects from both domain interfaces are important, consistent with the diffusion constant given above and hydrogen bond lifetime results. Attraction from both domain surfaces increases the water layer survival time compared to that near a single-domain surface.

Figure 8b shows the comparison of the layer survival correlation time for the first solvation shell versus the second

solvation shell (defined as $4\text{--}8 \text{ \AA}$ from surface here). The layer survival correlation time of the first solvation shell decays slower than that of the second solvation shell, indicating an enhanced immobility of water near the domain surface. The water molecules in the first solvation shell have comparable residence time for both $D = 12$ and 20 \AA cases, while the water molecules in the second solvation shell ($D = 12 \text{ \AA}$) have a residence time longer than that of the $D = 20 \text{ \AA}$ case, indicating that when $D = 12 \text{ \AA}$ the two domains still have influence on water molecules near the center of the interdomain region, which is also consistent with what has been observed in the diffusion constants (see Figure 3).

4. Conclusion

In this paper, we have studied the detailed water dynamics inside the interdomain region of a two-domain protein BphC enzyme in an effort to understand the effect of hydrophobicity and surface curvature on water dynamics. The results indicate that the dynamics of confined water in the interdomain region of a protein complex is slower than that of water near a single protein surface, and significantly slower than that of bulk water. The details are summarized as follows.

(1) The difference in the diffusion constant and water transit time can be a factor of as much as 2 depending on the distance from the interface. The presence of the hydrophobic protein surface slows the water dynamics in its solvation shells. The effect from both domain surfaces will slow the water dynamics even further compared to that at a single protein surface. This surface effect extends as far as 8 \AA from the interface in the interdomain region. However, when the domain–domain separation is further increased to 20 \AA , the water at the center of the interdomain region behaves like the bulk water. It is also found that different topologies of the two domain surfaces can influence the water dynamics as well.

(2) The hydrogen bonds of water molecules near the domain interface have longer relaxation times than those in the bulk. The hydrogen bonds between water molecules very close to the domain surfaces can persist ~ 3 times as long as the hydrogen bonds in the bulk. The effect from the two surfaces can extend as far as 8 \AA , in contrast to $4\text{--}5 \text{ \AA}$ from a single domain surface. When the contributions from pair diffusion are eliminated, a similar tendency is still observed.

(3) The radial distribution functions of water with respect to various protein atomic sites reveal the structural organization of water near the protein surface. The radial distribution functions around the polar atomic sites have a sharper first peak compared to those around the nonpolar atomic sites. The atomic sites in the concave regions have a broader distribution compared to the sites in the convex region.

(4) The residence times of water near surface atomic sites show that water molecules can persist for extremely long times near concave surfaces in the interdomain region, much longer than near the outside of convex surfaces, indicating that the local curvature can have a profound effect on water dynamics. On average, water molecules near hydrophilic surface regions have longer residence times than those near hydrophobic surface regions. It is also found that water layer survival time in the confined region between two domains is longer than it is near a single domain surface.

Acknowledgment. We thank Gerhard Hummer and Haiping Fang for helpful comments and discussions. This work was

partially supported by a grant to B.J.B. from the NIH (GM4330) and by a SUR Grant from IBM Corp. for an IBM LINUX CLUSTER.

References and Notes

- (1) Fersht, A. R. *Structure and Mechanism in Protein Science*; W. H. Freeman and Co.: New York, 1999.
- (2) Alberts, B.; Johnson, A.; Lewis, J.; Raff, M.; Roberts, K.; Walter, P. *Molecular Biology and the Cell*, 4th ed.; Taylor & Francis: New York, 2001.
- (3) Brooks, C. L.; Onuchic, J. N.; Wales, D. J. *Science* **2001**, 293, 612.
- (4) Dobson, C. M.; Sali, A.; Karplus, M. *Angew. Chem., Int. Ed.* **1998**, 37, 868.
- (5) Brooks, C. L.; Gruebele, M.; Onuchic, J. N.; Wolynes, P. G. *Proc. Natl. Acad. Sci. U.S.A.* **1998**, 95, 11037.
- (6) Cheng, Y.; Rossky, P. J. *Nature* **1998**, 392, 696.
- (7) Hummer, G.; Garde, S.; Garcia, A. E.; Pratt, L. R. *Chem. Phys.* **2000**, 258, 349.
- (8) Luzar, A.; Leung, K. *J. Chem. Phys.* **2000**, 113 (14), 5836.
- (9) Leung, K.; Luzar, A. *J. Chem. Phys.* **2000**, 113 (14), 5845.
- (10) Leung, K.; Luzar, A.; Bratko, D. *Phys. Rev. Lett.* **2003**, 90, 65502.
- (11) Lum, K.; Luzar, A. *Phys. Rev. E* **1997**, 56 (6), 6283.
- (12) Bizzarri, A. R.; Cannistraro, S. *J. Phys. Chem. B* **2002**, 106, 6617.
- (13) Li, J. Y.; Li, X.; Ye, L.; Chen, H. J.; Fang, H. P.; Wu, Z. H.; Zhou, R. *J. Phys. Chem. B* **2005**, 109, 13639.
- (14) Xu, H.; Berne, B. J. *J. Phys. Chem. B* **2001**, 105, 11929.
- (15) Levitt, M.; Park, B. H. *Structure* **1993**, 1, 223.
- (16) Karplus, P. A.; Faerman, C. *Curr. Opin. Struct. Biol.* **1994**, 4, 770.
- (17) Lee, C. Y.; McCammon, J. A.; Rossky, P. J. *J. Chem. Phys.* **1984**, 80, 4448.
- (18) Bagchi, B. *Chem. Rev.* **2005**, 105, 3197.
- (19) Bhattacharyya, S. M.; Wang, Z. G.; Zewail, A. H. *J. Phys. Chem. B* **2003**, 107, 13218.
- (20) Schoenborn, B. P.; Garca, A.; Knott, R. *Prog. Biophys. Mol. Biol.* **1995**, 64, 105.
- (21) Wanderlingh, J. N.; Giordano, R.; Sciortino, M. T.; Dianoux, A. J. *J. Phys. IV* **2000**, 10 (Part 7), 325.
- (22) Wiesner, S. K.; Prendergast, E.; Halle, B. *J. Mol. Biol.* **1999**, 286, 233.
- (23) Pal, S. K.; Peon, J.; Zewail, A. H. *Proc. Natl. Acad. Sci. U.S.A.* **2002**, 99, 1763.
- (24) Zhou, R.; Huang, X.; Margulius, C. J.; Berne, B. J. *Science* **2004**, 305, 1605.
- (25) Smolin, N.; Winter, R. *J. Phys. Chem. B* **2004**, 108, 15928.
- (26) Henchman, R. H.; Mccammon, J. A. *Protein Sci.* **2002**, 11, 2080.
- (27) Luise, A.; Falconi, M.; Desideri, A. *Proteins* **2000**, 39, 56.
- (28) Brunne, R. M.; Liepinsh, E.; Otting, G.; Wuthrich, K.; vanGunsteren, W. F. *J. Mol. Biol.* **1993**, 231, 1040.
- (29) Makarov, V. A.; Andrews, B. K.; Smith, P. E.; Pettitt, B. *Biophys. J.* **2000**, 79, 2966.
- (30) Weik, M. *Eur. Phys. J. E* **2003**, 12, 153.
- (31) Marchi, M.; Sterpone, F.; Ceccarelli, M. *J. Am. Chem. Soc.* **2002**, 124, 6787.
- (32) Huang, X.; Margulius, C. J.; Berne, B. J. *Proc. Natl. Acad. Sci. U.S.A.* **2003**, 100, 11953.
- (33) Huang, X.; Zhou, R.; Berne, B. J. *J. Phys. Chem. B* **2005**, 109, 3546.
- (34) Zhou, R.; Royyuru, A.; Athma, P.; Silverman, B. D. *Proteins* **2003**, submitted for publication.
- (35) Lindahl, E.; Hess, B.; van der Spoel, D. *J. Mol. Model.* **2001**, 7, 306.
- (36) Jorgensen, W. L.; Maxwell, D.; Tirado-Rives, J. *J. Am. Chem. Soc.* **1996**, 118, 11225.
- (37) Berendsen, H. J. C.; Postma, J. P. M.; van Gunsteren, W. F.; Hermans, J. *Intermolecular Forces*; B. Pullman Reidel: Dordrecht, The Netherlands, 1981.
- (38) Hess, B.; Bekker, H.; Berendsen, H. J. C.; Fraaije, J. G. E. M. *J. Comput. Chem.* **1997**, 18, 1463.
- (39) Risken, H., *The Fokker-Planck Equation*; Springer: Berlin, 1989.
- (40) Pu, L.; Harder, E.; Berne, B. J. *J. Phys. Chem. B* **2004**, 108, 6595.
- (41) Mahoney, M. W.; Jorgensen, W. L. *J. Chem. Phys.* **2001**, 114, 363.
- (42) Luzar, A.; Chandler, D. *Nature* **1996**, 379, 55.
- (43) Koneshan, S.; Rasaiah, J. C.; Lynden-Bell, R. M.; Lee, S. H. *J. Phys. Chem. B* **1998**, 102, 4193.
- (44) Garcia, A. E.; Stiller, L. *J. Comput. Chem.* **1993**, 14, 1396.
- (45) Rocchi, C.; Bizzarri, A. R.; Cannistraro, S. *Chem. Phys.* **1997**, 214, 261.
- (46) Muegge, I.; Knapp, E. W. *J. Phys. Chem.* **1995**, 99, 1371.
- (47) Rocchi, C.; Bizzarri, A. R.; Cannistraro, S. *Phys. Rev. E* **1998**, 57, 3315.
- (48) Gresh, D.; Suits, F.; Sham, Y. *IEEE Visualization 2001* **2001**, 445.
- (49) Humphrey, W.; Dalke, A.; Schulten, K. *J. Mol. Graphics* **1996**, 14, 33.